HHS Public Access

Author manuscript

J Aerosol Sci. Author manuscript; available in PMC 2018 August 01.

Published in final edited form as:

J Aerosol Sci. 2017 August ; 110: 25–35. doi:10.1016/j.jaerosci.2017.05.006.

In Vitro Assessment of Small Charged Pharmaceutical Aerosols in a Model of a Ventilated Neonate

Landon Holbrook[1,a], **Michael Hindle**[2], and **P. Worth Longest**[1,2,b]

[1]Department of Mechanical and Nuclear Engineering, Virginia Commonwealth University, Richmond, VA

[2]Department of Pharmaceutics, Virginia Commonwealth University, Richmond, VA

Abstract

Aerosolized medications may benefit infants receiving mechanical ventilation; however, the lung delivery efficiency of these aerosols is unacceptably low. *In vitro* experiments were conducted to evaluate aerosol delivery through conventional and modified ventilation systems to the end of a 3mm endotracheal tube (ETT) under steady state and realistic cyclic flow conditions. System modifications were employed to investigate the use of small charged particles and included streamlined components, a reduction in nebulizer liquid flow rate, synchronization with inspiration, and implementation of a previously designed low-flow induction charger (LF-IC), which was further modified in this study. Cyclic flow experiments implemented a modern ventilator with bias airflow and an inline flow meter, both of which are frequently excluded from *in vitro* tests but included in clinical practice. The modified LF-IC system demonstrated superior delivery efficiency to the end of the ETT (34%) compared with the commercial system (~1.3%) operating under cyclic ventilation conditions. These findings indicate that commercial systems still provide very low lung delivery efficiencies despite decades of innovation. In contrast, the modified system increased dose delivery to the end of the ETT by 26-fold. Despite initial concerns, the charged aerosol could be efficiently delivered through the small diameter ETT and reach the lungs. Future studies will be required to determine if the applied particle charge can eliminate expected high exhalation aerosol loss and will require the development of a realistic lung model.

Key terms

infants; pharmaceutical aerosols; mechanical ventilation; endotracheal tube; induction charger; respiratory drug delivery

[b]Corresponding author: Dr. P. Worth Longest, PhD, Virginia Commonwealth University, 401 West Main Street, P.O. Box 843015, Richmond, VA 23284-3015, Phone: (804)-827-7023, Fax: (804)-827-7030, pwlongest@vcu.edu.

[a]Current Address: Center for Environmental Medicine, Asthma, and Lung Biology, University of North Carolina at Chapel Hill, Chapel Hill, NC

Conflict of Interest Statement

No conflicts of interest exist.

1. Introduction

The extent to which poor lung delivery efficiency of aerosolized medicines limits treatment options for ventilated neonates and infants has been highlighted in numerous studies (Dubus et al., 2005; Fink 2004; Fok et al., 1996; Mazela and Polin 2011; Sidler-Moix et al., 2013). Overcoming this limitation and increasing the lung delivery efficiency of pharmaceutical aerosols are expected to improve the clinical effects of existing medications and expand the number of aerosol therapies available for infants in the future (Holbrook et al., 2015b). Aerosol delivery efficiencies in the range of <1–14% are common in mechanically ventilated infants, even considering more recent vibrating mesh nebulizer (VMN) devices (Dubus et al., 2005; Fink 2004; Fok et al., 1996; Mazela and Polin 2011; Sidler-Moix et al., 2013). In addition to very low aerosol delivery efficiencies, high deposition variability is also a likely reason for poor biological response when infants receive aerosolized medicines (Mazela and Polin 2011; Shah et al., 2007). Small diameter connective ventilator tubing, short inhalation periods, and small tidal volumes all contribute to ineffective aerosol delivery to ventilated infants (Fink 2004; Rubin and Fink 2001). A significant challenge to aerosol delivery during mechanical ventilation is passing the aerosol through the gas delivery tubing, connection components and patient interface device. Ventilation components are typically designed for gas delivery, not aerosol administration (Longest et al., 2014a; Longest et al., 2014b). In addition to this, the nebulizer type, location within the ventilation circuit, gas flow, and mode of nebulizer operation are important considerations for increasing aerosol delivery efficiency during mechanical ventilation (Fink and Ari 2013). Much work is still needed to improve aerosol delivery efficiency and reduce intersubject variability in mechanically ventilated infants, so that the clinical benefit of existing medications can be maximized and new inhaled therapies can be developed (Brion et al., 2006; Cole et al., 1999; Fink 2004; Rubin and Williams 2014; Shah et al., 2007).

Through the use of VMNs and new ventilation connection components, aerosol delivery efficiency has recently been improved in models of ventilated infants. A macaque animal model of a ventilated infant was used to demonstrate a lung delivery efficiency of 12.6 – 14% of the aerosolized dose through a 3 mm infant endotracheal tube (ETT) using a VMN synchronized with inspiration and without ventilator bias flow (Dubus et al., 2005). Using a jet nebulizer in an *in vitro* model of a ventilated premature infant, with a new connector to separate nebulizer and ventilation gas bias flow, Mazela et al. (2014) increased albuterol sulfate delivery efficiency from 1% or less through the commercial Y-connector to a maximum of approximately 7% with the improved connector, before the ETT or mask. Additional aerosol losses are known to occur in the infant ETT, which can have an internal diameter as small as 2.5 mm. Similar to the 12.6–14% *in vivo* animal lung model delivery efficiency predictions of Dubus et al. (2005), Longest et al. (2014b) used *in vitro,* whole lung, and CFD modeling techniques to predict the lung deposition fraction for a newborn full-term infant under mechanical ventilation through an ETT using commercial connection components (6.8 – 13.5%). A new streamlined Y-connector was then implemented with synchronized delivery and reduced droplet sizes (~ 1.8 μm) to improve aerosol deposition in the infant lungs (Longest et al., 2014b). For a full term (3.6 kg) infant and 3 mm ETT,

maximum total lung delivery efficiency of a polydisperse aerosol with a mass median aerodynamic diameter (MMAD) of 1.8 μm reached 45.2%.

A “small” aerosol with a MMAD of 1.6 μm has been produced with a “high” net charge of approximately 1% of the Rayleigh limit with the intention of reducing the depositional losses before the patient, increasing the mass of drug that reaches the patient, and decreasing the exhaled fraction of the drug (Holbrook et al., 2015b). This was accomplished using a novel low flow-induction charger (LF-IC) that incorporated a commercial VMN with a reduced mass output and counter-electrode to produce a charged aerosol through induction charging. The current work will begin with this previously developed LF-IC applied in an infant ventilation circuit containing a 3 mm endotracheal tube during steady state flow conditions and then under cyclic flow conditions.

The purpose of charging the aerosol is to reduce ventilation losses that occur when small particles enter the lungs, lack sufficient inertia and mass to deposit, and are then exhaled. Longest et al. (2014b) predicted that these ventilation losses were as high as 40% of the nebulized dose for an infant with a small particle aerosol, even when the delivered dose was synchronized with inhalation. One potential strategy to reduce these ventilation losses is to provide an electrostatic charge to the particles or droplets. Deposition arising from charge is proportional to both conduit diameter and particle or droplet residence time. In theory, the charged aerosol will pass quickly through the ETT and upper airways with insufficient time for depositional loss to increase. As the aerosol penetrates the bifurcating lung network, velocities are reduced and sufficient time is available to increase deposition from electrostatic charge, thereby reducing ventilation losses and increasing aerosol retention in the lungs. However, it is not clear if the charged aerosol can effectively penetrate the nebulizer system and small diameter ETT without large increases in deposition loss.

The objective of this study is to compare the performance of a newly developed LF-IC system to that of a commercially available nebulizer system in an infant ventilation circuit under steady-state and cyclic flow conditions. The LF-IC and commercial device performances are evaluated by the quantification of albuterol sulfate (AS; model drug) mass recovered using high performance liquid chromatography (HPLC) in multiple system components (Figure 1). After implementing the previously developed LF-IC in an infant ventilation circuit under idealized steady-state airflow, the LF-IC is redesigned to minimize device volume for use with cyclic flow conditions and to allow for the inclusion of a ventilator flow meter (Schena et al., 2015), a new common feature in mechanical ventilation systems that has not adequately been considered in previous studies. This redesigned LF-IC also incorporates a breath actuated nebulizer to increase delivery of aerosolized drug to the patient and reduce the exhaled dose.

2. Materials and Methods

2.1. Overview of Systems

In this study, commercial and modified aerosol delivery systems were compared for full term neonates receiving invasive mechanical ventilation. Both systems utilized a VMN to produce the test aerosol. The commercial system included a commercial T-connector,

commercial Y-connector, and a continuous nebulization signal operating the VMN (Figure 1a). The modified delivery system included a reduced nebulizer signal to reduce liquid mass output and promote evaporation of the droplets, breath synchronized nebulizer timing, introduction of a streamlined low flow-induction charger (LF-IC) (Holbrook et al., 2015a), and a streamlined Y-connector (Figure 1b) (Longest et al., 2014b). Two flow conditions were evaluated with each system, steady state and cyclic ventilation. Steady state flow conditions allow for simplified and idealized experiments to be conducted at the same flow rates of previous characterization studies (Holbrook et al., 2015b). The cyclic flow condition better represents clinical use and *in vivo* aerosol delivery during invasive mechanical ventilation. Cases considered are presented in Table 1. Briefly, Systems with 1.* and 2.* designations indicate steady state and cyclic ventilation conditions, respectively. The second number in the designation indicates changes in the charging voltage, run time, nebulization signal, and nebulization timing. An additional case was considered to evaluate the effects of extended run times and the potential for static charge buildup on insulated ventilation components. Elements of the delivery systems and flow conditions are described in the following paragraphs.

The nebulization signal to the VMN (Aeroneb Lab; Aerogen Limited, Galway, Ireland) was altered in some systems (Table 1) to reduce the momentum of the aerosol stream and to reduce the aerosol droplet mass flow rate entering the airstream. The reduced momentum was expected to reduce depositional loss in the LF-IC. The reduced aerosol droplet mass flow rate allowed for evaporation of the nebulized droplets to achieve a small size (MMAD) and this was expected to reduce losses in the ventilator components and 3 mm ETT (Teleflex Medical; Research Triangle Park, NC). Drug mass deposition in system components and on the filter (Pulmoguard II filter; Quest Medical; Brockton, MA), indicative of lung delivered dose, was quantified for the commercial and modified systems using high performance liquid chromatography (HPLC). The nebulizer solution formulation contained 0.25%$^{w}/_{v}$ AS (Spectrum Chemicals, New Brunswick, NJ; model drug commonly used as a bronchodilator) and 0.25% $^{w}/_{v}$ NaCl in water. The volume of nebulized liquid solution was determined by weighing the nebulizer before and after nebulization and using an assumed density of 1 g/ml. The nominal delivered dose of AS was calculated by multiplying the volume of nebulized formulation (mL) by the concentration of AS in the solution (0.25%$^{w}/_{v}$). The methods for fabrication and use of the original LF-IC with an AS and sodium chloride solution can be found in the study of Holbrook et al. (2015b).

To expand upon initial evaluations with steady state flow conditions, the current study also includes analysis during realistic cyclic ventilation. The cyclic ventilation flow condition was generated by a Galileo ventilator (Hamilton Medical Inc; Reno, NV) and a Model 1601 Adult/Infant Training/Test Lung (Michigan Instruments; Grand Rapids, MI) to simulate the full invasive ventilation breathing cycle (inhalation, exhalation, and breath pause). Expansion to cyclic ventilation required two new components in the flow circuit, which are the ventilator's flow meter (Figure 2) and the exhalation filter (which attaches to the exhalation outlet of the Y-connector shown in Figure 1b). Aerosol that has insufficient mass and charge to deposit in the lungs would be captured by the ventilator exhalation filter. Both of these necessary components (flow meter and exhalation filter) provide additional sources of aerosol loss that will be analyzed in this study.

The impact of the ventilator flow meter (Figure 2), which is required for most modern ventilators to properly function, on aerosol delivery to ventilated patients has not been adequately assessed in the literature. Many ventilators, such as the one used in the current study, utilize an inline flow meter containing a screen with small holes which cannot be removed from the ventilator circuit due to feedback controls and patient alarms. These flow meters are needed due to the importance of monitoring the ventilated volume to reduce the incidence of ventilator induced lung injury (Slutsky 2015). The flow meter measures both inspiratory and expiratory flow and is positioned after the Y-connector in the single limb connected to the ETT.

Under cyclic ventilation conditions, the commercial delivery setup with a VMN (System 2.1) was compared with a charged small aerosol setup (System 2.2). Two key changes for delivering the charged small aerosol were the use of a reduced volume LF-IC positioned between the flow meter and ETT, and synchronization of the nebulizer timing with inhalation (Table 1). This synchronization is controlled by two electrical relays that are triggered by the breathing pattern of the infant ventilator. Further details of the reduced volume LF-IC redesign and experimental testing methods for these systems are described in the following sections and summarized in Table 1.

2.2. Steady State Flow Condition

Aerosol delivery during 5 LPM steady state flow is quantified in an infant ventilation circuit consisting of commercial components, i.e., System 1.1. As in all cases considered, drug mass deposition was determined in each component of the system by separate washings in deionized water and determining the concentration with HPLC using validated techniques as described in the study of Holbrook et al. (2015b). Depositional accumulation of droplets on the walls of the nebulizer in the commercial system caused dripping into the T-connector, necessitating the grouping of nebulizer and T-connector in the drug mass determination. To retain consistency across the systems, this procedure was also followed for the LF-IC, even though the aerosol did not accumulate in the nebulizer and drip into the LF-IC. With System 1.1, the aerosol first enters the commercial neonatal T-connector (Aerogen Limited) where it is entrained in the 5 LPM supply air. It then passes into a commercial Y-connector (included in a neonatal conventional ventilation circuit, (Teleflex Medical; Research Triangle Park, NC)) that has the exhalation port sealed. The nebulizer is positioned as close as possible to the Y-connector. The outlet of the Y-connector is attached directly to an uncuffed ETT, which is curved through a 90 degree bend with a 3 cm radius of curvature, representing passage through the infant oropharyngeal region (Longest et al., 2014b). The ETT has an inner diameter of 3 mm and an outer diameter of 4 mm, consistent with use in a full-term neonate. The outlet of the ETT is positioned inside a Pulmonguard II filter and is less than one centimeter from the filter surface inside the filter plastic housing to enhance impaction and total capture of the aerosol. The connection between ETT and filter is open to atmosphere to allow different airflow through the ventilation components and the filter. A steady state flow of 5 LPM was pushed through the system using a compressed gas source, while 20 LPM was pulled through the filter using a downstream vacuum pump intended to completely capture the aerosol exiting the ETT during the 0.5 minute experiment. A summary of the critical components in System 1.1 is shown in Figure 3a. The particle size

distribution for the Aeroneb Lab nebulizer operated at 5 LPM was previously reported in Longest et al. (2014b) and had a mass median aerodynamic diameter (MMAD) of 4.9 (standard deviation; SD = 0.3) μm.

To improve aerosol delivery, streamlining (Longest et al., 2014a), induction charging (Golshahi et al., 2015), and reduced nebulization output (resulting in the modified system) were evaluated under steady state flow conditions, i.e., System 1.2. The experimental setup for System 1.2 was the same as Figure 3a, but with the LF-IC replacing the commercial T-connector and a streamlined Y-connector replacing the commercial infant version. The VMN driving signal was modified to produce a sinusoidal waveform with an amplitude of 32.4 volts peak-to-peak (VPP) and a frequency of 128.2 kHz to reduce the emitted dose and the initial momentum of the nebulized aerosol. The modified signal had a dose output that was $1/10^{th}$ the commercial system but a much higher expected delivery efficiency, such that the runtime for System 1.2 was increased from 0.5 minutes to 1 minute to ensure sufficient drug mass was available for HPLC quantification. In addition to comparing commercial nebulization with the LF-IC under steady state conditions, the operating duration of System 1.2 (1 minute) was increased to 30 minutes in System 1.3 to examine the accumulation of charged droplets depositing on the insulated components over time. HPLC analysis and nominal dose calculation methods were unchanged from the study of Holbrook et al. (2015b). Based on previous measurements (Holbrook et al., 2015b), the LF-IC at an airflow rate of 5 LPM and reduced nebulizer output produced an aerosol with a MMAD (SD) of 1.6 (0.1) μm. At an induction charger voltage of 1 kV, elementary charges at midpoint diameters of 0.79, 1.29, and 2.02 μm were 170, 514, and 1590 e, which were approximately 1% of the Raleigh charge limit, and were 10 fold higher than without charging (Holbrook et al., 2015b).

2.3. Commercial Delivery System during Cyclic Ventilation

A Galileo ventilator was implemented to supply realistic invasive mechanical ventilation conditions, and was set to provide pressure controlled constant mandatory ventilation (P-CMV). Positive end-expiratory pressure (PEEP) was set to 5 cm H_20 and $P_{control}$ was set to 15 cm H_20 resulting in a peak inspiratory pressure (PIP) of 20 cm H_20. The rise time for pressure in a pressure controlled setting, P_{ramp}, was set to 100 ms. The number of breaths per minute was set to 30. Each 2 second breath was composed of 0.6 seconds of inspiration and 1.4 seconds of expiration, giving an I:E ratio of 1:2.3. These choices were consistent with target parameters for a 3.55 kg infant as specified by Walsh & DiBlasi (2010) and are summarized in Table 2.

The Galileo ventilator has a positive constant bias inflow (or bias flow) that is intended to purge the exhaled gas and reduce patient re-breathing of CO_2. For cyclic ventilation, the ETT was inserted and sealed into a Pulmoguard II filter with the filter housing outlet attached to the training test lung (TTL) operating in infant mode. The resistance and compliance of the TTL were selected to have values of 20 cm H_20/L/sec and 0.002 L/cm H_20, respectively. Resistance and compliance value selection was based on the study of Abbasi et al. (2012). The cyclic flow conditions have an additional filter at the exhalation outlet of the Y-connector to capture the exhaled dose as shown in Figure 3b and 3c. The

commercial cyclic ventilation setup, System 2.1, was run for one minute with continuous nebulization (Table 1).

2.4. Modified Delivery System during Cyclic Ventilation

To reduce the loss of drug due to bias flow and to avoid excessive deposition on the flow meter, the commercial system was modified by redesigning the LF-IC and changing its position (Figure 3c). The nebulizer was moved from the inspiratory line to after the Y-connector. The LF-IC was redesigned for use in System 2.2 due to the relocation closer to the patient (Figure 2). The redesigned LF-IC had a reduced internal volume to minimize gas re-breathing associated with the low tidal volume of air. The original LF-IC with the 45 mL air space was acceptable in the inspiratory line because the bias-flow prevented re-breathing of exhaled gasses. The new reduced volume LF-IC shown in Figure 2 is streamlined to seamlessly connect the ventilator flow meter, Aeroneb Lab nebulizer, and the 3 mm ETT. The internal volume of the LF-IC is now 6.7 mL. This reduced downstream volume is necessary to minimize re-breathing considering that a 45 mL device placed after the Y-connector would prevent effective ventilation of an infant having a tidal volume of approximately 28 mL. The distance between the induction electrode and the nebulizer's mesh surface is decreased from 47.6 to 46.0 mm. The induction charging voltage is also decreased from 1 kV to 0.5 kV to minimize loss on the induction electrode. A summary of parameters defining System 2.2 is provided in Table 1.

In this study, breath synchronized nebulization is utilized to reduce the amount of aerosol that is being lost during the exhalation portion of the breathing cycle. The Galileo ventilator has an internal relay that can be used to trigger an external nebulizer for delivery of aerosol during inspiratory flow or expiratory flow. A standard external Multifunction Timer Relay (Finder Relays, INC.; Suwanee, GA) was operated in On-Delay mode and connected in series with the internal relay to allow for a delayed trigger from the beginning of inspiration or expiration (Figure 4). The time delay was adjusted to trigger the nebulizer 1.29 seconds after the beginning of expiration, and that is 0.11 seconds before inspiration (Figure 5). The duration of nebulization was 0.11 seconds. These values were based on a preliminary optimization study (data not reported) that considered both the length of nebulization and the best nebulization start time evaluated at multiple time points in the inhalation and exhalation breathing periods. A 20 volt DC signal is provided by a laboratory DC power supply (Tenma Test Equipment; Springboro, OH) to the internal Galileo relay such that during expiration, the 20 volt signal is sent to the on-delay relay, and during inspiration no signal is present at the on-delay relay.

2.5 Statistical Analysis

A one-way analysis of variance (ANOVA) was conducted to compare the effects of the different study devices (Devices 1.1, 1.2 and 1.3) on the regional deposition of drug. Post hoc analysis was performed using Tukey-Kramer HSD test. A paired t-test was used to compare Systems 2.1 and 2.2. Significance was assessed at the level of $P<0.05$. All experiments were conducted with at least n=3 replicates.

3. Results

3.1. LF-IC Performance during Steady State Flow

The LF-IC (System 1.2) is compared with the commercial setup (System 1.1) under steady-state conditions to determine mass balance of the delivered dose, locations of aerosol deposition, and delivery rate of drug through the ETT to the filter. To establish delivered dose mass balance, the total amount of drug recovered from the system components and filter was divided by the calculated nominal dose for Systems 1.1 and 1.2, respectively, resulting in mean (and coefficient of variation, CV; based on n=3 replicates) values of 97.3 % (2.6 %) and 95.2 % (2.7 %) drug recovery during steady-state flow. The mean (SD) amount of drug recovered from the commercial nebulizer outlet and T-connector was 59.9 (1.5) % (System 1.1) of the recovered dose, while the modified System 1.2 had a significantly lower drug deposition (22.2 (5.3) %; P=0.0025; Tukey-Kramer HSD) in the LF-IC (nebulizer outlet and streamlined T-connector; Figure 6). Aerosol deposition in the commercial Y-connector was 12.7 (3.0) % of the AS mass recovered. The streamlined Y-connector contained 4.9 (0.7) % of the deposited aerosol, which was significantly lower than the commercial Y (P=0.007; Tukey-Kramer HSD). In both systems, about 17% of the drug mass was deposited in the ETT and was not significantly different. The commercial setup, System 1.1, achieved 10.0 (2.6) % delivery of the AS aerosol to the lung filter, while System 1.2 achieved 48.9 (6.4) % delivery of the charged aerosol to the lung filter (P=0.01; Tukey-Kramer HSD). These findings are shown graphically in Figure 6, where error bars represent +/− 1 standard deviation (SD).

Having determined the regional deposition of the aerosolized AS, the total mass emitted from the nebulizer (μg) and rate of drug delivery to the filter (μg/min) were calculated for Systems 1.1 and 1.2. The mean (CV) emitted dose of AS (n = 3) in the commercial and modified setups was 976.4 μg (5.8 %) and 128.7 μg (11.2 %), respectively. The commercial system demonstrated a drug delivery rate of 156.0 μg/min (33.3 %) to the lung filter. The LF-IC's drug delivery rate in the modified system was 67.7 μg/min (15.5%) to the lung filter. Again, both systems were considered at a steady state 5 LPM airflow. The LF-IC had approximately 50% of the commercial setup drug delivery rate to the lung filter, but improved delivery efficiency to the lung filter by 5-fold and improved variability by reducing the CV of the delivery rate by a factor of 2-fold.

3.2. Effect of Delivery Time in a Charged Aerosol System

The LF-IC was run for 30 minutes at the same steady state air flow rate of 5 LPM using the same nebulizer formulation as considered with Systems 1.1 and 1.2 to examine the effect of static charge buildup associated with increased runtime (i.e., System 1.3). With the 30 minute run, the mean (SD) drug mass as a percentage of total recovery in the nebulizer and T-connector was 24.2 (12.3) %. Under the 30 minute run conditions, the streamlined Y-connector had 5.9 (1.6) % of the recovered drug mass. Both of these depositional losses were significantly lower compared with the deposition observed using System 1.1 (P<0.05; Tukey-Kramer HSD). The ETT captured 21.7 (17.0) % of the recovered drug mass. The efficiency of the LF-IC in delivering drug to the filter was 48.2 (17.2)% over the 30 minute run compared to 48.9 (6.4)% for the same conditions and a 1 minute run. The drug delivery

rate to the lung filter was 67.5 (38.2) μg/min over 30 minutes with a total recovered mass of 4182.6 (4.2) μg in the system. The overall recovery of drug was 99.0 (0.9) % of the nominal dose indicating excellent mass balance. A comparison of System 1.2 (1 minute run time) and System 1.3 (30 minute run time) is provided in Figure 7. Based on these findings, there does not appear to be a build-up of static charge over a 30 minute run that can influence depositional loss in the system.

3.3. LF-IC Performance during Cyclic Ventilation

As with Systems 1.1 to 1.3, System 2.1 and System 2.2 are evaluated to determine recovery mass balance, aerosol deposition location, and rate of drug mass delivery to the inhalation filter. Mean (CV) recovered drug expressed as a percentage of the nominal dose for commercial System 2.1 was 94.1 % (3.5%) and for the modified and charged System 2.2 was 101.2 % (2.4%) under cyclic ventilation conditions. Evaluation under realistic cyclic flow conditions allows for measurement of the mean (SD) drug that is exhaled before it enters the patient, in the commercial [16.2 (3.7) %] and the modified [18.6 (1.7) %] systems, which were not significantly different (t-test). The mean (SD) loss of drug in the commercial Y-connector is 7.9 (3.4) % of the recovered dose. This is in contrast to the loss in the streamlined Y-connector using the LF-IC, which was significantly lower (1.2 (0.5) %; P=0.04; t-test). The ventilator's flow meter captured 4.8 (3.9) % of the drug in the commercial system and 4.0 (0.4) % of the drug in the modified system. The nebulizer and T-connector contained 67.6 (4.3)% of the recovered AS in the commercial system, while 25.2 (2.8)% was in the nebulizer and reduced volume LF-IC in the modified system (P=0.0004; t-test). Drug mass recoveries in the ETT were significantly different for the commercial and modified systems with values of 1.7 (1.6) and 17.1 (1.0)%, respectively (P=0.0004; t-test). The lung filter captured 1.3 (0.6)% of the recovered AS in the commercial system and 34.0 (1.7)% of the recovered AS in the charged and modified system indicating a statistically significant 26-fold improvement in drug delivery efficiency (P=0.0003; t-test). These results for cyclic ventilation are summarized in Figure 8. The lung filter delivery efficiencies of Systems 1.1 through 2.2 are summarized in Table 3 and used to compare efficiencies across all the systems in the Discussion.

The commercial system delivered 25.6 μg/min of AS to the lung filter under cyclic ventilation conditions (System 2.1) with a CV of 41.4%. The modifications applied to the LF-IC caused the modified setup (System 2.2) to deliver 3.5 μg/min of AS to the lung filter with a CV of 3.7%. 2043.5 μg/min of AS was nebulized in System 2.1 and 10.4 μg/min AS was nebulized in System 2.2. As a result, for a realistic cyclic ventilation condition, the modified system reduced drug delivery rate 7-fold, improved drug delivery efficiency to the lung filter 26-fold, and reduced the lung delivery variability (CV) 11-fold.

Discussion

In the study of Holbrook et al. (2015b), a novel aerosol generation system was designed and selected to produce a small charged aerosol with a mass median aerodynamic diameter (MMAD) in the range of 1–2 μm. This approximate size was chosen to minimize deposition in the ventilation circuitry and ETT (Longest et al., 2014b), while the charge was added to

reduce the exhalation of the small aerosol inhaled by the patient. *In vitro* testing of the novel LF-IC system in mechanical ventilation circuits was conducted in this study to verify the reduction in losses due to reduced MMAD and ensure the induced charge on the aerosol did not counteract the benefits associated with smaller particle size and streamlined designs.

For a commercial VMN and system evaluated under cyclic flow conditions, this study predicts that the total drug mass delivered to the end of the ETT (lung filter) is approximately 1.3% of the nebulized dose (Table 3). This result is much lower than the 12.6 to 14 % lung deposition efficiency reported in the study of Dubus et al. (2005), which considered deposition of an aerosol produced by a breath synchronized VMN in four intubated macaques. One major difference in these two studies is that Dubus et al. (2005) used a ventilator without an inline flow meter and without bias flow. All of the 25 ventilators (from 10 different manufacturers) reviewed by Schena (2015) contain inline flow meters. Future mechanical ventilators will likely continue the current trend of increasing patient monitoring and feedback control based on various meters allowing for improved ventilation synchrony (Kacmarek 2011). The modern Galileo ventilator used in this study is more consistent with current and likely future mechanical ventilation practice than previous studies which often do not include flow meters or bias-flow, and is therefore an accurate assessment of maximum mesh nebulizer performance in current clinical scenarios. It should be remembered that this and previous *in vitro* studies neglect a majority of the exhaled dose (that which enters the lung and does not deposit), so the predicted lung filter dose is a maximum estimate of lung deposition efficiency.

This study maximized lung delivery during cyclic flow using a new reduced volume LF-IC positioned downstream of the Y-connector with a modified signal and synchronization with breathing. For the modified system under cyclic flow, System 2.2, a charged aerosol enters a region with an electric field and zero airflow 0.11 seconds prior to inhalation producing 25.2% deposition of the nebulized aerosol in the charging region. The remaining fraction is then transported by the inhalation flow through the ETT, where a fraction of the aerosol deposits, reducing the potential inhaled fraction. 34.0% of the aerosol is deposited in the lung filter, leaving the remaining 24% that does not reach the filter to be exhaled through the ETT (Table 3). Previous work has shown that approximately 60% delivery efficiency to the lung was possible using numerical modeling and accounting for the lung exhaled dose; but nebulizer and T-connector deposition was neglected based on the optimized systems developed by Longest et al. (2014b). If nebulizer and T-connector deposition is added to the lung filter deposition for System 2.2, 59.2% deposition is estimated. This excellent agreement highlights the need for future studies to further reduce system losses and implement previously optimized designs (Longest et al., 2014b). The nebulizer relocation, signal modification, and breath synchronization of delivery contributed to a 26-fold increase in inhaled dose in the modified system compared with a VMN commercial system (34.0% vs. 1.3%).

Initial experiments (not reported here) showed very low inhaled dose when the LF-IC was upstream of the Y-connector under cyclic ventilation. Redesigning and moving the LF-IC downstream of the Y-connector and the flow meter reduced depositional loss during inspiration, decreased the dead volume to increase efficiency, and demonstrated the large

influence of nebulizer positioning within the circuit. The charged aerosol in this study likely decreases the amount delivered to the inhalation filter, but in future studies that consider the complete lung, a charged aerosol is expected to enhance lung deposition and reduce lung exhaled dose. Initial experiments also showed a large influence of delivery timing as various durations and starting times of nebulization were explored before selecting a nebulizer duration of 0.11 seconds synchronized to occur 0.11 seconds prior to inhalation. The exhaled fraction can be viewed as the fraction of drug that could be gained by reducing dead volume or improving synchronization of nebulization. Additional optimization of breath synchronization timing may increase the delivery rate, perhaps without decreasing the delivery efficiency. Future work will need to consider timing aerosol generation to begin during exhalation, but continue into the beginning of inspiration. This will require better ventilator control of the attached nebulizer or additional hardware such as a “true-off/on delay”. This additional hardware would allow for control of the activation and duration of nebulization as opposed to only controlling the onset or activation of the nebulizer and using the change of breath phase to turn off the device. Further improvement is possible to deliver more aerosol in a shorter amount of time.

The device volume has been reduced through redesign, but the filter still provides a large dead volume of air that may artificially reduce the capabilities of both the commercial and LF-IC systems. This effect was minimized by placing the tip of the ETT very near the filter media. The enlarged dead volume of the system means that generated aerosol will still be in the line after inhalation and a portion will remain after exhalation. Clinically, dead volume is a critical quantity that must be minimized to reduce the amount of re-breathing of exhaled gas a patient incurs. The current positioning of the LF-IC downstream of the flow meter is not current clinical practice, but viewed as acceptable in this and other studies when the residual volume of the nebulizer is small (Ari and Fink 2015; Dhand 2008; Duarte et al., 2001).

Drug delivery rate to the lung filter in the commercial system decreased from 156 μg/min to 25.6 μg/min due to the cyclic breathing profile, ventilator flow meter deposition, and bias flow (System 1.1 vs. 2.1). The delivery rate of modified Systems 1.2 vs. 2.2 decreased from 67.7 μg/min to 3.5 μg/min, primarily due to the reduced nebulization time of the synchronized nebulizer, i.e., 0.11 seconds spraying time for every 2 second breath. The reduced delivery rate of the synchronized LF-IC also has an 11.2 fold reduction of CV from 41.4% (System 2.1) to 3.7% (System 2.2). As described previously, an advantage of the LF-IC is a 26-fold improvement in delivery efficiency of the nebulized aerosol to the lungs, but the LF-IC is also shown here to be more consistent. These improvements are critical for providing efficient and reproducible lung delivery of therapeutic aerosols.

In designing this system for delivering aerosolized pharmaceuticals, medications that have high cost (e.g. surfactants) and unwanted secondary effects (e.g. steroids) are being primarily considered. Albuterol sulfate is inexpensive, has low side effects, does not require a large dose, and may therefore be acceptable using the inefficient and highly variable devices that are currently available. The LF-IC is then ideally positioned to deliver drugs such as surfactants, antibiotics, and steroids (as well as others) because the emphasis of design is on efficiency and reproducibility rather than speed. Even with the reduced drug

delivery rate of the LF-IC, the reduction in variability allows for equivalent dosing with low variability when the patient is treated for a longer time. Clinical trials of aerosol delivery of some inhaled medications have had inconclusive or mixed outcomes likely due to high variability and poor lung delivery efficiency (Berggren et al., 2000; Finer et al., 2010).

The steady state system uses dry (RH < 6%) room temperature air flowing through the system at 5 LPM, while the cyclic system utilizes a heater to maintain an approximately 35° Celsius inspiratory line. A humidifier was not connected in the cyclic ventilation system; rather the patient is reliant on the liquid content of the evaporating aerosolized droplets in the heated line to prevent the cooling and drying of the airways by dry and cold ventilation gas. Dubus et al. (2005), who provides the current benchmark of *in vivo* delivery in macaques with 3 mm ETTs, did not use a system with added heat or humidity. Additionally, the ventilator that was used by Dubus et al. did not have bias flow or an in-line flow meter (Dubus et al., 2005). Bias flow, humidity, and position of aerosol device in the circuit, are expected to be important factors for improving aerosol delivery efficiency during mechanical ventilation (Ari and Fink 2015). The system considered in this study delivers humidity through the nebulization of an aqueous solution to avoid dehydrating the airways (Ari and Fink 2015). Using a heated and humidified line, Mazela et al. (2014) delivered 6.6% of a nominal AS dose to the end of the Y-connector in a mechanical ventilation system; however, an ETT was not considered. This system used a novel VC connector to bypass bias flow and improve delivery of a jet nebulizer providing a drug delivery rate of 2.9 μg/min (Mazela et al., 2014).

In conclusion, the LF-IC system was found to increase the lung dose delivery efficiency during steady state ventilation from 10.0% to 48.9% and during cyclic ventilation from 1.3% to 34.0%. This 26-fold increase in the lung dose efficiency of the LF-IC over the commercial system during invasive mechanical ventilation is expected to be maintained in clinical trials. The induced charge on the aerosol from the LF-IC is expected to enhance deposition in the small diameter infant airways, while the commercial aerosol which reaches the lungs will likely be exhaled at a higher fraction. The variability in the delivered lung dose using commercial delivery under steady state flow (System 1.1) was 26% and decreased to 13% in the modified system under steady-state flow (System 1.2). In the cyclically ventilated systems, the variability decreased from 46.2% in the commercial system (System 2.1) to 5% in the modified system (System 2.2). Based on the superior efficiency performance (26 fold improvement of inhaled dose) and the reduced variability (1/10 CV of delivery rate) of the LF-IC system compared with the commercial system during realistic cyclic flow, further testing and implementation of the new LF-IC system in clinical or highly realistic *in vitro* models is suggested.

Acknowledgments

Research reported in this publication was supported by the Eunice Kennedy Shriver National Institute of Child Health & Human Development of the National Institutes of Health under Award Number R21HD073728. The content is solely the responsibility of the authors and does not necessarily represent the official views of the National Institutes of Health.

References

Abbasi S, Sivieri E, Roberts R, Kirpalani H. Accuracy of tidal volume, compliance, and resistance measurements on neonatal ventilator displays: An in vitro assessment. Pediatric Critical Care Medicine. 2012; 13(4):e262–e268. [PubMed: 22596072]

Ari A, Fink JB. Aerosol Drug Delivery During Mechanical Ventilation: Devices, Selection, Delivery Technique, and Evaluation of Clinical Response to Therapy. Clinical Pulmonary Medicine. 2015; 22(2):79–86.

Berggren E, Liljedahl M, Winbladh B, Andreasson B, Cursted T, Robertson B. Pilot study of nebulized surfactant therapy for neonatal respiratory distress syndrome. Acta Paediatr. 2000; 89(4):460–464. [PubMed: 10830460]

Brion LP, Primhak RA, Yong W. Aerosolized diuretics for preterm infants with (or developing) chronic lung disease. Cochrane Database Of Systematic Reviews. 2006; (3)

Cole CH, Colton T, Shah BL, Abbasi S, MacKinnon BL, Demissie S, Frantz ID. Early inhaled glucocorticoid therapy to prevent bronchopulmonary dysplasia. New England Journal Of Medicine. 1999; 340(13):1005–1010. [PubMed: 10099142]

Dhand R. Aerosol delivery during mechanical ventilation: From basic techniques to new devices. Journal of Aerosol Medicine and Pulmonary Drug Delivery. 2008; 21(1):45–60. [PubMed: 18518831]

Duarte AG, Fink JB, Dhand R. Inhalation therapy during mechanical ventilation. Respir Care Clin N Am. 2001; 7(2):233–60. vi. [PubMed: 11517022]

Dubus JC, Vecellio L, De Monte M, Fink JB, Grimbert D, Montharu J, Valat C, Behan N, Diot P. Aerosol deposition in neonatal ventilation. Pediatric Research. 2005; 58(1):10–14. [PubMed: 15774850]

Finer NN, Merritt TA, Bernstein G, Job L, Mazela J, Segal R. An open label, pilot study of Aerosurf combined with nCPAP to prevent RDS in preterm neonates. Journal of Aerosol Medicine and Pulmonary Drug Delivery. 2010; 23(5):303–309. [PubMed: 20455772]

Fink J, Ari A. Aerosol delivery to intubated patients. Expert opinion on drug delivery. 2013; 10(8): 1077–1093. [PubMed: 23614495]

Fink JB. Aerosol delivery to ventilated infant and pediatric patients. Respiratory Care. 2004; 49(6): 653–665. [PubMed: 15165300]

Fok TF, Monkman S, Dolovich M, Gray S, Coates G, Paes B, Rashid F, Newhouse M, Kirpalani H. Efficiency of aerosol medication delivery from a metered dose inhaler versus jet nebulizer in infants with bronchopulmonary dysplasia. Pediatric Pulmonology. 1996; 21(5):301–309. [PubMed: 8726155]

Golshahi L, Longest PW, Holbrook L, Snead J, Hindle M. Produciton of highly charged pharmaceutical aerosols using a new aerosol induction charger. Pharmaceutical Research. 2015 in review.

Holbrook L, Hindle M, Longest PW. Generating charged pharmaceutical Aerosols intended to improve targeted drug delivery in ventilated Infants. Journal of Aerosol Science. 2015a:35–47. [PubMed: 26273108]

Holbrook L, Hindle M, Longest PW. Generating charged pharmaceutical aerosols intended to improve targeted drug delivery in ventilated infants. Journal of Aerosol Science. 2015b; 88:35–47. [PubMed: 26273108]

Kacmarek RM. The mechanical ventilator: past, present, and future. Respiratory care. 2011; 56(8): 1170–1180. [PubMed: 21801579]

Longest PW, Azimi M, Golshahi L, Hindle M. Improving aerosol drug delivery during invasive mechanical ventilation with redesigned components. Respiratory Care. 2014a; 59(5):686–698. [PubMed: 24106320]

Longest PW, Azimi M, Hindle M. Optimal delivery of aerosols to infants during mechanical ventilation. Journal of Aerosol Medicine and Pulmonary Drug Delivery. 2014b; 27(5):371–385. [PubMed: 24299500]

Mazela J, Chmura K, Kulza M, Henderson C, Gregory TJ, Moskal A, Sosnowski TR, Florek E, Kramer L, Keszler M. Aerosolized albuterol sulfate delivery under neonatal ventilatory conditions:

In vitro evaluation of a novel ventilator circuit patient interface connector. Journal of Aerosol Medicine and Pulmonary Drug Delivery. 2014; 27(1)

Mazela J, Polin RA. Aerosol delivery to ventilated newborn infants: historical challenges and new directions. Eur J Pediatr. 2011; 170:433–444. [PubMed: 20878336]

Rubin BK, Fink JB. Aerosol therapy for children. Respir Care Clin N Am. 2001; 7(2):175–213. [PubMed: 11517020]

Rubin BK, Williams RW. Emerging aerosol drug delivery strategies: From bench to clinic. Advanced drug delivery reviews. 2014; 75:141–148. [PubMed: 24993613]

Schena E, Massaroni C, Saccomandi P, Cecchini S. Flow measurement in mechanical ventilation: a review. Medical engineering & physics. 2015; 37(3):257–264. [PubMed: 25659299]

Shah V, Ohlsson A, Halliday HL, Dunn MS. Early administration of inhaled corticosteroids for preventing chronic lung disease in ventilated very low birth weight preterm neonates. Cochrane Database Of Systematic Reviews. 2007; (4)

Sidler-Moix AL, Dolci U, Berger-Gryllaki M, Pannatier A, Cotting J, Di Paolo ER. Albuterol Delivery in an In Vitro Pediatric Ventilator Lung Model: Comparison of Jet, Ultrasonic, and Mesh Nebulizers. Pediatric Critical Care Medicine. 2013; 14(2):E98–E102. [PubMed: 23287904]

Slutsky AS. History of Mechanical Ventilation. From Vesalius to Ventilator-induced Lung Injury. American journal of respiratory and critical care medicine. 2015; 191(10):1106–1115. [PubMed: 25844759]

Walsh, BK., DiBlasi, RM. Mechanical ventilation of the neonate and pediatric patient. In: Walsh, BK.Czervinske, MP., DiBlasi, RM., editors. Perinatal and Pediatric Respiratory Care. Saunders Elsevier; St. Louis: 2010. p. 325-347.

Highlights

- Aerosol delivery to an infant lung model using a modern ventilator
- Lung aerosol delivery efficiency for a commercial system was 1.3%
- Modifications included streaming and synchronization
- Modifications increased lung delivery efficiency to 34%

The small charged aerosol could be efficiently delivered to the lungs

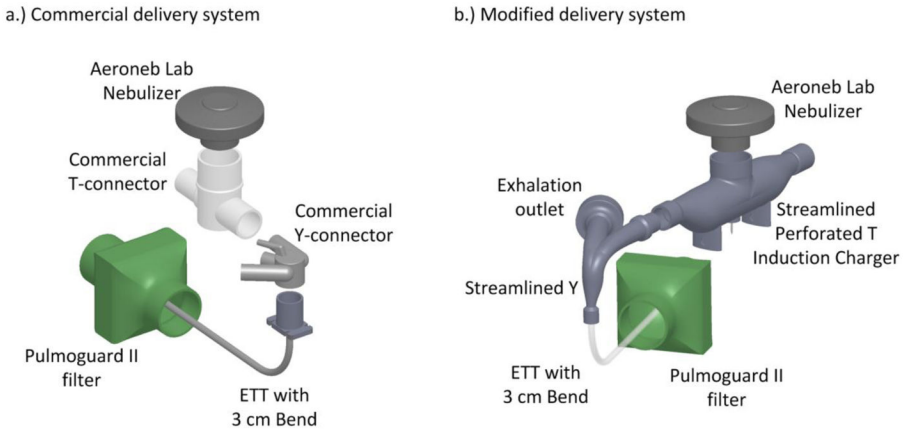

Figure 1.

Aerosol delivery through the (a) commercial delivery system and (b) modified delivery system. Both the T-connector and the Y-connector are streamlined in the modified delivery system.

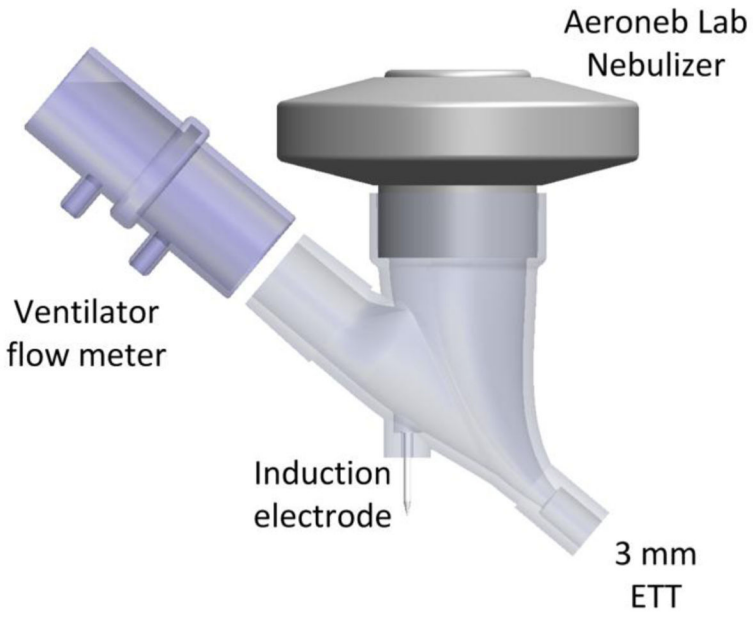

Figure 2.
Streamlined low flow induction charger (LF-IC) with reduced volume located after the flow meter. This T-connector was used in the System 2.2 cyclic ventilation experiments.

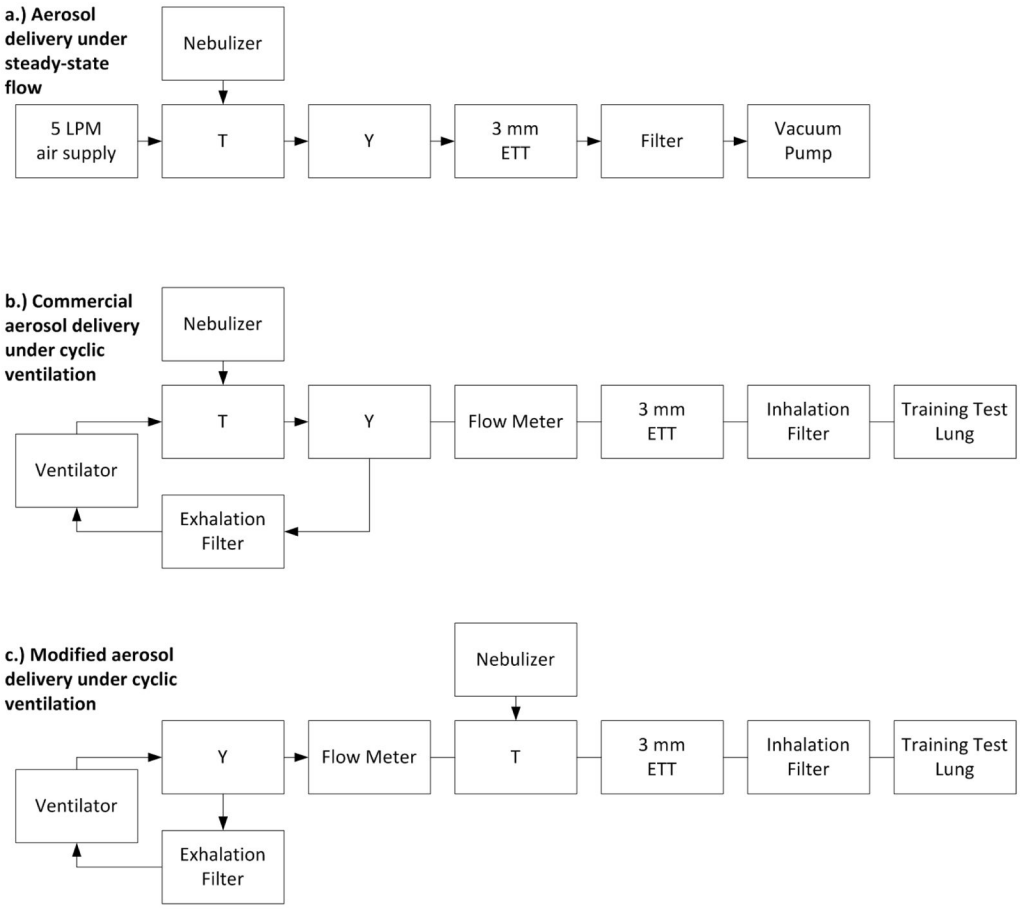

Figure 3.

Connection configuration for (a) aerosol delivery under steady-state flow (commercial and modified systems), (b) commercial aerosol delivery system under cyclic ventilation, and (c) modified aerosol delivery system under cyclic ventilation.

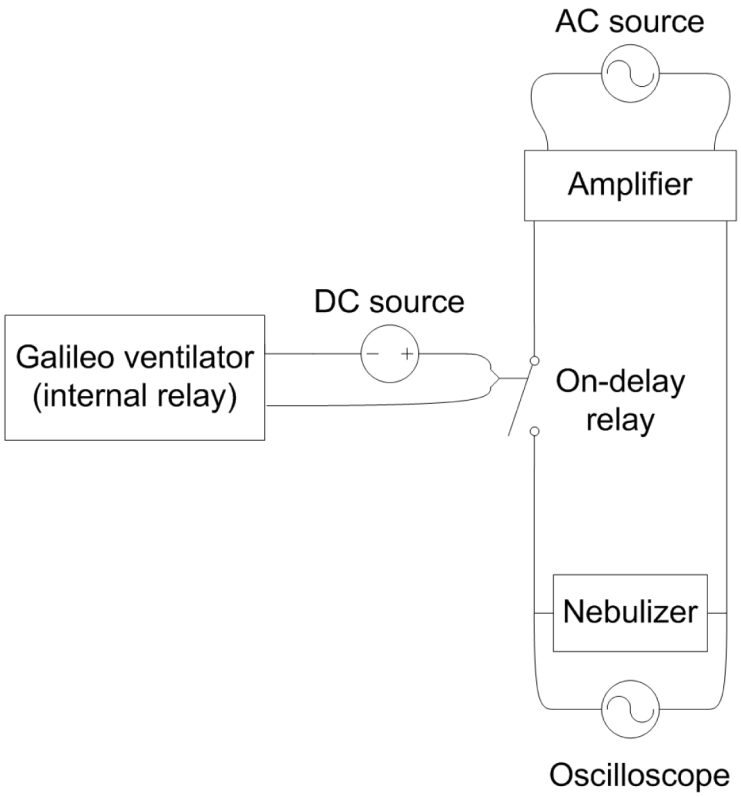

Figure 4.
Electrical wiring diagram for the modified LF-IC system under cyclic ventilation conditions (System 2.2).

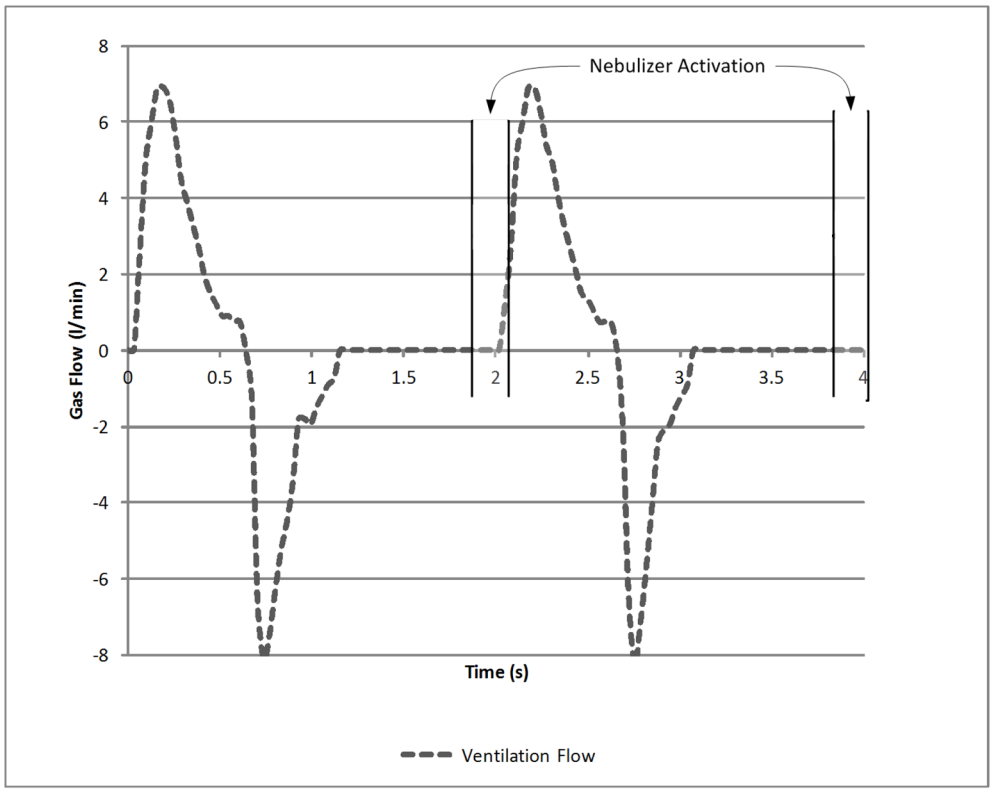

Figure 5.

Flow profile resulting from pressure control ventilation ($P_{control}$ = 15, PEEP = 5, P_{ramp} = 100 ms) with timing of aerosol generation (synchronized nebulization) 0.11 seconds prior to inhalation.

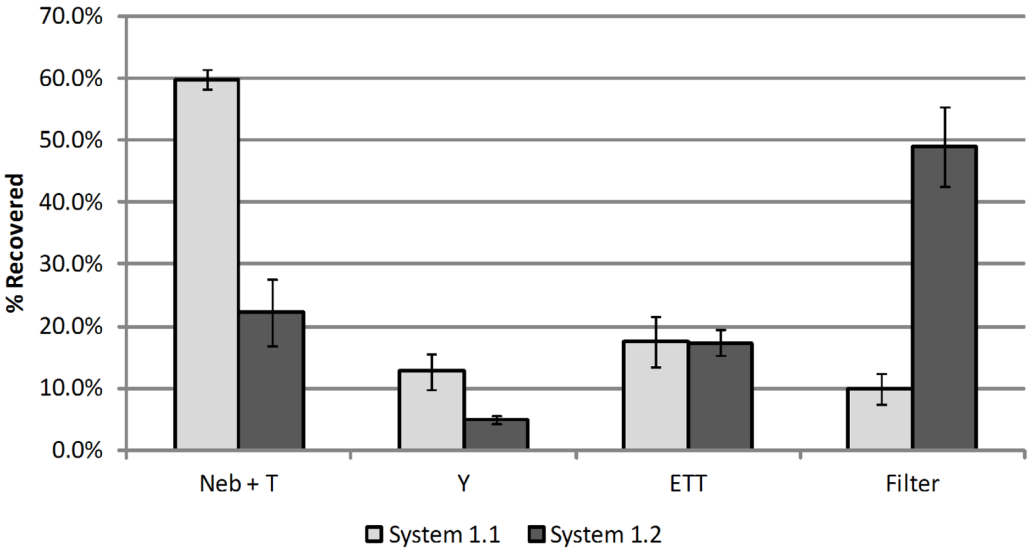

Figure 6.

Drug mass deposition efficiency (% based on recovered drug) in ventilator circuit under steady-state flow during operation of System 1.1 (commercial) and System 1.2 (modified with streamlined components & 1 kV charge) with n = 3 for each system; error bars represent standard deviation.

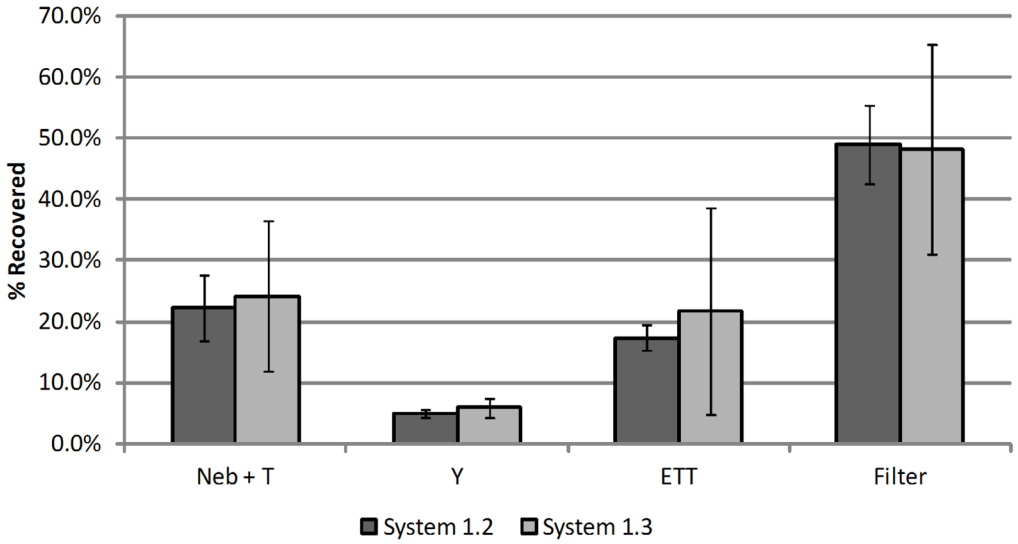

Figure 7.

Effect of operating time on drug mass deposition efficiency (% based on recovered drug) in ventilator circuit under steady-state flow during operation of streamlined & 1 kV charged LF-IC Systems 1.2 and 1.3 (n = 3 for each system; error bars represent standard deviation).

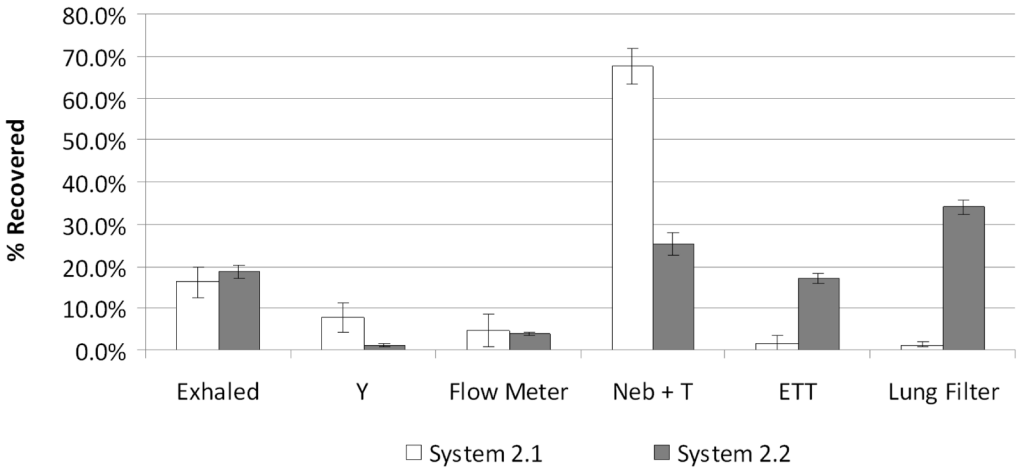

Figure 8.

Drug mass deposition efficiency (% based on recovered drug) for System 2.1 and 2.2 under cyclic flow conditions with error bars representing standard deviation (n = 3). System conditions are defined in Table 1.

Table 1

Overview of systems considered. Designation with 1.* indicates steady state flow conditions and 2.* represents cyclic ventilation. Commercial cases are Systems 1.1 and 2.1.

System	T and Y Connector Streamlining	Air-flow Conditions	Charging Voltage (kV)	Runtime (min)	Nebulization Signal	Nebulization Timing
1.1	Commercial	Steady	0	0.5	Commercial	Continuous
1.2	Streamlined[a]	Steady	1	1	32.4 VPP[c]	Continuous
1.3	Streamlined[a]	Steady	1	30	32.4 VPP[c]	Continuous
2.1	Commercial	Cyclic	0	1	Commercial	Continuous
2.2	Streamlined[b]	Cyclic	0.5	20	32.4 VPP[c]	0.11 (s) before inhale

[a] Implements the LF-IC (Figure 1b)

[b] Implements the reduced volume LF-IC (Figure 2)

[c] VPP: Peak-to-Peak Voltage

Table 2

Ventilation parameters to represent invasive mechanical ventilation of a full term neonate (3.55 kg) based on Walsh & DiBlasi (2010).

Ventilation Parameters	
$P_{control}$	15 cm H20
PEEP	5 cm H20
P_{ramp}	100 ms
Ventilation Mode	P-CMV
Breath/Min	30
T_{insp}	0.6 s

Table 3

Drug mass deposited in each system component as a percentage of total recovered dose (and standard deviation; SD). Exhaled drug mass and deposition in the Y-connector, flow meter, Neb + T, and ETT all represent sources of drug loss. Lung filter deposition represents an approximation of the drug delivery efficiency to the lungs.

System	1.1	1.2	1.3	2.1	2.2
Exhaled	N/A	N/A	N/A	16.2 (3.7) %	18.6 (1.7) %
Y-Connector *	12.7 (3.0) %	4.9 (0.7) % **	5.9 (1.6) % **	7.9 (3.4) %	1.2 (0.5) % ***
Flow Meter	N/A	N/A	N/A	4.8 (3.9) %	4.0 (0.4) %
Neb + T *	59.9 (1.5) %	22.2 (5.3) % **	24.2 (12.3) % **	67.6 (4.3) %	25.2 (2.8) %
ETT	17.5 (4.1) %	17.4 (2.2) %	21.7 (17.0) %	1.7 (1.6) %	17.1 (1.0) % ***
Lung Filter *	10.0 (2.6) %	48.9 (6.4) % **	48.2 (17.2) % **	1.3 (0.6) %	34.0 (1.7) % ***
Total Loss [1]	90.0 (2.6) %	44.4 (7.0) % **	51.8 (17.2) % **	98.2 (0.6) %	66.0 (1.7) % **

[1] Defined as the aerosol depositing on components other than the lung filter.

* Significant effect of device (1.1, 1.2. and 1.3) on drug deposition (P<0.05; ANOVA)

** Significant difference compared to device 1.1 (P<0.05; Tukey-Kramer HSD)

*** Significant difference compared to device 2.1 (P<0.05; t-test)